Electrospray mass spectral study of isopolyoxomolybdates †

Daud K. Walanda, Robert C. Burns, Geoffrey A. Lawrance and Ellak I. von Nagy-Felsobuki *

Department of Chemistry, The University of Newcastle, Callaghan, NSW 2308, Australia.
E-mail: chvo@cc.newcastle.edu.au. Fax: 61-2-49215472

Electrospray mass spectrometry (ESMS) has been performed on aqueous solutions of dilute (10^{-3} M) isopoly-oxomolybdate systems. There is direct evidence that the evaporation process in the ESMS technique involves significant chemical effects, resulting in the detection of many new anions and cations. For ammonium poly-oxomolybdate systems, negative-ion ESMS yields ions of the form $[HMo_mO_{3m+1}]^-$, $[Mo_mO_{3m+1}]^{2-}$, $[Mo_mO_{3m+2}]^{4-}$ as well as $[Mo_7O_{24}]^{6-}$, whereas for alkali metal polyoxomolybdate systems ions of the form $[Mo_mO_{3m+1}A]^-$ and $[Mo_mO_{4m}A_{2m-2}]^{2-}$ (where A = Li$^+$, Na$^+$ or K$^+$) were observed. In positive-ion mode two series of polyoxomolybdate cations, namely $[Mo_mO_{4m}A_{2m+1}]^+$ and $[Mo_mO_{4m}A_{2m+2}]^{2+}$ could be assigned. Aggregates of both the $[HMo_mO_{3m+1}]^-$ and $[Mo_mO_{3m+1}]^{2-}$ series in the ammonium polyoxomolybdate system can be classified in terms of open-chained structures of tetrahedra that are corner shared, whereas the highly charged anions $[Mo_mO_{3m+2}]^{4-}$ and $[Mo_mO_{3m+3}]^{6-}$ are consistent with closed-packed structures. For the alkali metal polyoxomolybdate anion and cation systems the spectra are consistent with open-chained structures of octahedral units that are edge shared, with a terminating tetrahedral unit. Linear correlations suggest that the assembly of these aggregates occurs *via* an addition polymerization mechanism. This model, consistent with the ESMS data, may identify the additive moieties (MoO_3, MoO_2^{2+} and $Mo_2O_8A_4$) required for aggregation of polyoxomolybdate species in aqueous solution.

The chemistry of molybdenum(VI) oxo-complexes has been investigated for several decades because of its importance in biochemical and chemical applications.[1–4] To exemplify this diversity, $[SiMo_{12}O_{40}]^{4-}$ has been used as an electron acceptor in studies of photosynthesis and photophosphorylation, whereas the mixed metal polyanions $[PV_xMo_{12-x}O_{40}]^{n-}$ coupled with palladium(II) salts have been used to catalyse the aerial oxidation of olefins.[2,3]

It is well known that in alkaline solution molybdate is present as the monomeric anion $[MoO_4]^{2-}$. However, on acidification polymerization occurs which leads to the formation of a range of isopolyoxomolybdate species. The polymerization reaction is thought to proceed mainly *via* condensation following protonation.[2–5] This yields isopolyoxomolybdate ions in aqueous solution of the form $[H_{p-2r}Mo_qO_{4q-r}]^{(2q-p)-}$, where p and q are the number of moles of H$^+$ and $[MoO_4]^{2-}$ in the reaction scheme respectively and r is the number of moles of water product. Hence each polyoxomolybdate species can be expressed according to the ratio H$^+$:$[MoO_4]^{2-}$. However, there is uncertainty concerning the speciation and formulation of some isopolyoxomolybdate species in solution, since they are difficult to characterize under such conditions.[6–16]

Several studies of alkali metal molybdates have confirmed that the monomolybdate $[MoO_4]^{2-}$ has a tetrahedral structure in both the solid state and in solution.[17,18] On addition of acid, $[MoO_4]^{2-}$ is protonated to yield $[HMoO_4]^-$ and subsequently H_2MoO_4.[17,19] The $[HMoO_4]^-$ and $[MoO_4]^{2-}$ ions are the predominant species at high pH ($> \approx 6$) and low concentration.[19] However, it has been suggested that $[HMoO_4]^-$ is probably octahedral due to an expansion of the co-ordination sphere[20–22] and some investigators[22–24] have proposed that $[HMoO_4]^-$ and

H_2MoO_4 are more appropriately designated as $[MoO(OH)_5]^-$ and $Mo(OH)_6$ respectively.

Investigations of the structures of isopolyoxomolybdates by Knöpnadel *et al.*[25] and Armour *et al.*[26] have shown that the crystal structure of $(NH_4)_2Mo_2O_7$ contains an infinite chain anion in which there are present both MoO_4 tetrahedra and MoO_6 octahedra. In contrast, the discrete $[Mo_2O_7]^{2-}$ anion consists of two corner-shared MoO_4 tetrahedra,[27] while Cooper and Salmon[28] have shown that the $[Mo_4O_{13}]^{2-}$ anion is a flexible chain of four linked MoO_4 tetrahedra. The $[Mo_6O_{19}]^{2-}$ anion was first identified and analysed structurally by Allcock *et al.*,[29] but in this case the building block of the structure is formed from six distorted MoO_6 octahedra that are condensed so that all share a common vertex.[30] Lindqvist[16,31] originally reported the structures of both the $[Mo_7O_{24}]^{6-}$ and $[Mo_8O_{26}]^{4-}$ anions, which consist of seven or eight MoO_6 edge-shared octahedra, respectively. The large $[Mo_{36}O_{112}(H_2O)_{18}]^{8-}$ anion has also been structurally characterized,[32] and consists of two octadeca-molybdate (18-molybdate) sub-units related to each other by a center of inversion. The structure involves both six- and seven-co-ordinated molybdenum atoms, while the co-ordinated water molecules are bound directly to the molybdenum atoms in both terminal and bridging locations. The structures of alkali metal isopolyoxomolybdates with general formula $[Mo_mO_{3m+1}A_2]$ (where A is an alkali metal ion and m is a positive integer) have also been investigated over the past two decades.[33] Structural studies have shown that the shapes of these compounds depend on the number of molybdenum atoms, m, and the size of the counter cation.[34]

Electrospray mass spectrometry (ESMS) has displayed its utility in characterizing polyoxometalates dissolved in organic, aqueous–organic and purely aqueous solutions.[35–38] The first ESMS study of dilute aqueous oligomeric anions was that of Howarth and co-workers,[38] who investigated aqueous solutions of isopolytungstates, peroxotungstates and heteropolymoly-bdates. Their study detected new species which had not been previously reported in water, including $[W_6O_{19}]^{2-}$ and $[W_2O_7]^{2-}$.

For mixed-metal species, heteropolyoxoanion species of the form $[H_xPW_nMo_{12-n}O_{40}]^{(3-x)-}$ were also reported. Moreover, Howarth and co-workers[38] were able to show that desolvation by the drying agent may lead to interference in the equilibrium process, since it rapidly changes the pH and concentrations of the solutes in the eventual formation of the analytes. Hence species extremely sensitive to either condition (*i.e.* presence of other species or pH) may differ in concentration from bulk measurements (where changes in such conditions are less rapid).

A number of investigations have been performed on poly-oxomolybdates using organic solvents. For example, Colton and Traeger[35] have shown that negative ion ESMS was amenable to analysing intact heteropolymolybdate species such as the $[S_2Mo_{18}O_{62}]^{2-}$ ion in acetonitrile. Similarly, Le Quan Tuoi and Muller[36] and Siu and co-workers[37] were successful in identifying the intact ions of heteropolyacids and polyoxoanions. They found that the negative-ion mass spectral data observed were in agreement with their respective calculated isotopic mass distributions. The study of Le Quan Tuoi and Muller[36] on hetero-polyacids in different solvents (*i.e.* methanol–water and acetonitrile–water) found anion peaks associated with the mono-, di- and tri-anions of $[H_3PMo_{12}O_{40}]$, $[H_4PMo_{11}VO_{40}]$, $[H_3PW_{12}O_{40}]$ and $[H_4SiW_{12}O_{40}]$. Siu and co-workers[37] performed experiments using ES tandem mass spectrometry on similar compounds as well as on a number of tetrabutyl-ammonium salts of the isopolyoxometalates (both molybdates and tungstates) in either acetone or methanol–water mixtures. They observed the parent ions $[Mo_2O_7]^{2-}$, $[Mo_6O_{19}]^{2-}$ and $[Mo_8O_{26}]^{4-}$ and fragment ions such as $[Mo_2O_7]^{2-}$, $[Mo_3O_{10}]^{2-}$, $[Mo_4O_{13}]^{2-}$ and $[Mo_5O_{16}]^{2-}$.

As an extension of our previous studies on the kinetics and mechanism of formation of heteropolyoxomolybdates[39–41] we report here the ESMS study of ammonium and alkali metal isopolyoxomolybdates in aqueous solution. The aggregates, which have been characterized by ESMS, are important to delineate the chemistry and suggest possible structures of the isopolyoxomolybdates.

Experimental

Sample preparation

Only lithium and ammonium molybdate compounds were synthesized. The other compounds in the series were available commercially [*e.g.* sodium molybdate, $Na_2MoO_4 \cdot 2H_2O$ (Univar, 99%), ammonium paramolybdate, $(NH_4)_6Mo_7O_{24} \cdot 4H_2O$ (Univar, 99%) and potassium molybdate, K_2MoO_4 (Aldrich, 98%)].

The ammonium molybdate was prepared by the action of aqueous NH_3 on $(NH_4)_6Mo_7O_{24}$. Three grams of $(NH_4)_6Mo_7O_{24} \cdot 4H_2O$ were dissolved in 20 mL of deionized water. To this solution was added, dropwise, a solution of concentrated NH_3. The mixture was stirred vigorously with a motor stirrer to release NH_3 gas. On standing for several days at room temperature colorless crystals precipitated. The product was recrystallized from water. IR spectrum: ν(N–H) 3100m, δ(NH$_2$) 1409s, ν(Mo–O) 839s cm^{-1}.

The lithium molybdate was prepared by the action of LiOH· H_2O on MoO_3. Equimolar proportions of reagent grade $LiOH \cdot H_2O$ (5.04 g) and MoO_3 (8.64 g) were mixed in 30 mL of deionized water. The resultant syrupy solution was allowed to stand for some days. The colorless crystalline product, Li_2MoO_4, was isolated and recrystallized from water. IR spectrum: ν(Mo–O) 833s cm^{-1}.

A Hanna HI 8521 pH meter (Hanna Instruments, Italy) was used for measuring pH values. It was calibrated at room temperature using buffers of pH 4.0 and 7.0 (BDH, Australia). Sample solutions were prepared by dissolving the colorless crystals in deionized water. The ESMS mobile phase was of similar pH to that of the sample solutions. The concentration

of all sample solutions was 10^{-3} M. A solution of 0.1% acetic acid was added to adjust the pH of each solution and the mobile phase to 4.5. A solution of pH 6.0 was prepared by boiling the deionized water and bubbling a stream of nitrogen gas through it while it cooled. The solutions were infused directly into the electrospray source by a 10 µL syringe assisted by the flow of the mobile phase (which was fed by a binary pump into the HPLC system).

Mass spectrometry

All the ESMS experiments were performed on a VG Platform II single quadrupole mass spectrometer (Micromass Ltd., Altrincham, UK) coupled to a HPLC binary pump system. For all spectral acquisitions, the tip of the capillary was at a potential of +3.5 and −3.5 kV relative to ground for positive-ion and negative-ion mode respectively. The source temperature was maintained at 353 K. The mobile phase consisted of water with appropriate concentrations of acetic acid. An optimum flow rate of 10 µL min^{-1} was employed. The cone voltage, CV, was varied between ±20 and ±60 V relative to the skimmer (which was set to ground). Raising the sample CV increases the collisional energy, which in turn enhances the formation of daughter ions by collisions with solvent molecules within the rotary-pumped region between the sample cone and the skimmers (focus cone and skimmer plate), or between the skimmers and RF lens (the hexapole).[35] A Rheodyne injector fitted with a 10 µL loop was used to inject the sample solution into the flow of the mobile phase.

Mass spectra were acquired by scanning the quadrupole mass filter from *m/z* 1500 to 100 and ions were detected by means of a scintillator detector. Approximately 25 scans were summed to give a mass spectrum. For the calibration spectra, a 3.0 µg µL^{-1} NaI solution was used with a 50:50 mixture of water and acetonitrile as the mobile phase. In positive-ion mode the spectrum exhibited sodium iodide clusters of the form $[Na_xI_y]^+$ (where $y = x - 1$), whereas in negative-ion mode sodium iodide clusters of the form $[Na_xI_y]^-$ (where $y = x + 1$) were used. All data were acquired and processed using the Micromass MassLynx system.

Results

In the negative-ion investigation of the $(NH_4)_6Mo_7O_{24}$ and $(NH_4)_2MoO_4$ solutions, members of three ion series were observed, namely $[HMo_mO_{3m+1}]^-$ (where $m = 1$ to 6), $[Mo_mO_{3m+1}]^{2-}$ (where $m = 2$ to 20) and $[Mo_mO_{3m+2}]^{4-}$ (where $m = 9$ to 23 and is only odd), as well as $[Mo_7O_{24}]^{6-}$.

Figs. 1 and 2 are typical of the spectra of ammonium poly-oxomolybdate solutions at pH 4.5 and 6.0 respectively for CV −20 and −60 V. The inserts of Figs. 1(a) and 2(a) show the quadruply charged series of isopolyoxomolybdates (*i.e.* the $[Mo_mO_{3m+2}]^{4-}$ species) at CV −20 V for pH 4.5 and 6.0 respectively. The inserts of Figs. 1(b) and 2(b) show the higher members of the $[Mo_mO_{3m+1}]^{2-}$ series and the $[Mo_7O_{24}]^{6-}$ ion respectively. The $[MoO_3]^-$ anion, formally containing Mo^V, is assigned as a fragment ion since it only appears when the CV is set at −60 V. Notably, the $[HMoO_4]^-$ anion is the most abundant peak in nearly all sample solutions. A detailed assignment for all isopolyoxomolybdate species is given in Table 1.

The negative-ion spectra of the alkali metal polyoxomoly-bdate systems are given in Fig. 3. Apart from the most abundant ion (*i.e.* $[HMoO_4]^-$), two series were observed which have the form $[Mo_mO_{3m+1}A]^-$ and $[Mo_mO_{4m}A_{2m-2}]^{2-}$ (where A = Li$^+$, Na$^+$ or K$^+$). The detailed assignments of the ESMS data for both CV −20 and −60 V at pH 4.5 are given in Table 2. Data measured at CV −20 and −60 V at pH 6.0 are available as SUP 57467.

In the positive-ion mode investigations of the ammonium and lithium polyoxomolybdate systems only a background signal was observed at pH 4.5 and 6.0 when the CV was set to
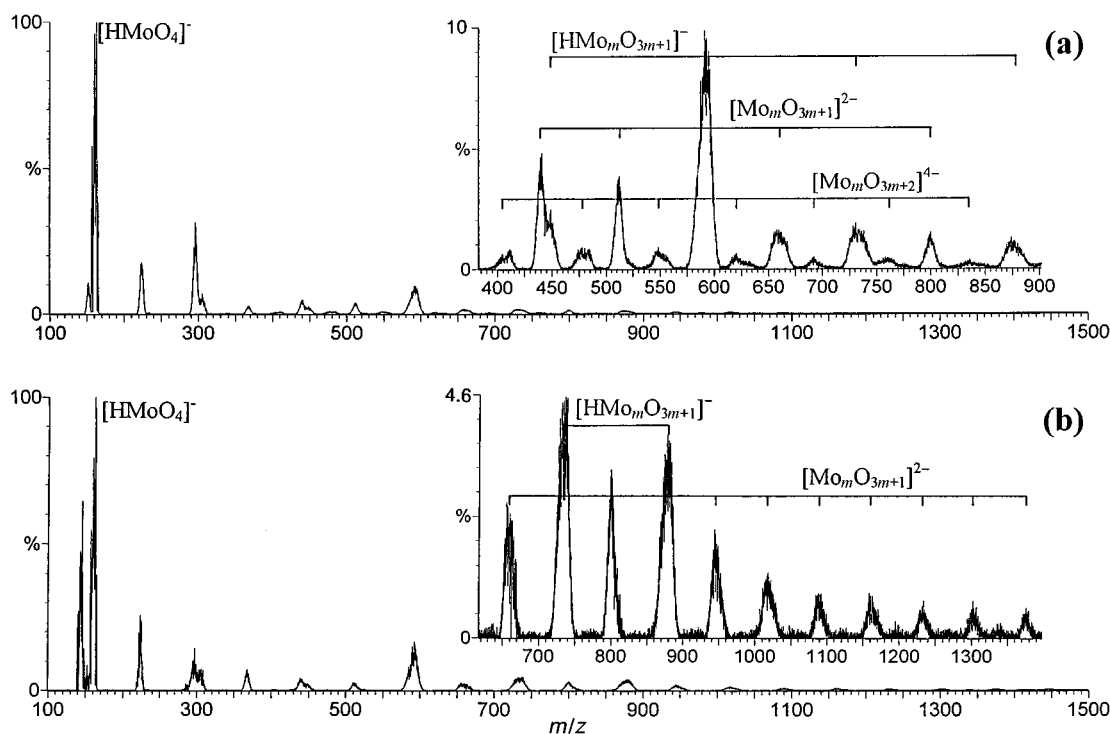
Fig. 1 Negative-ion ESMS of ammonium molybdate at pH 4.5: (a) CV set at -20 V; (b) CV set at -60 V.
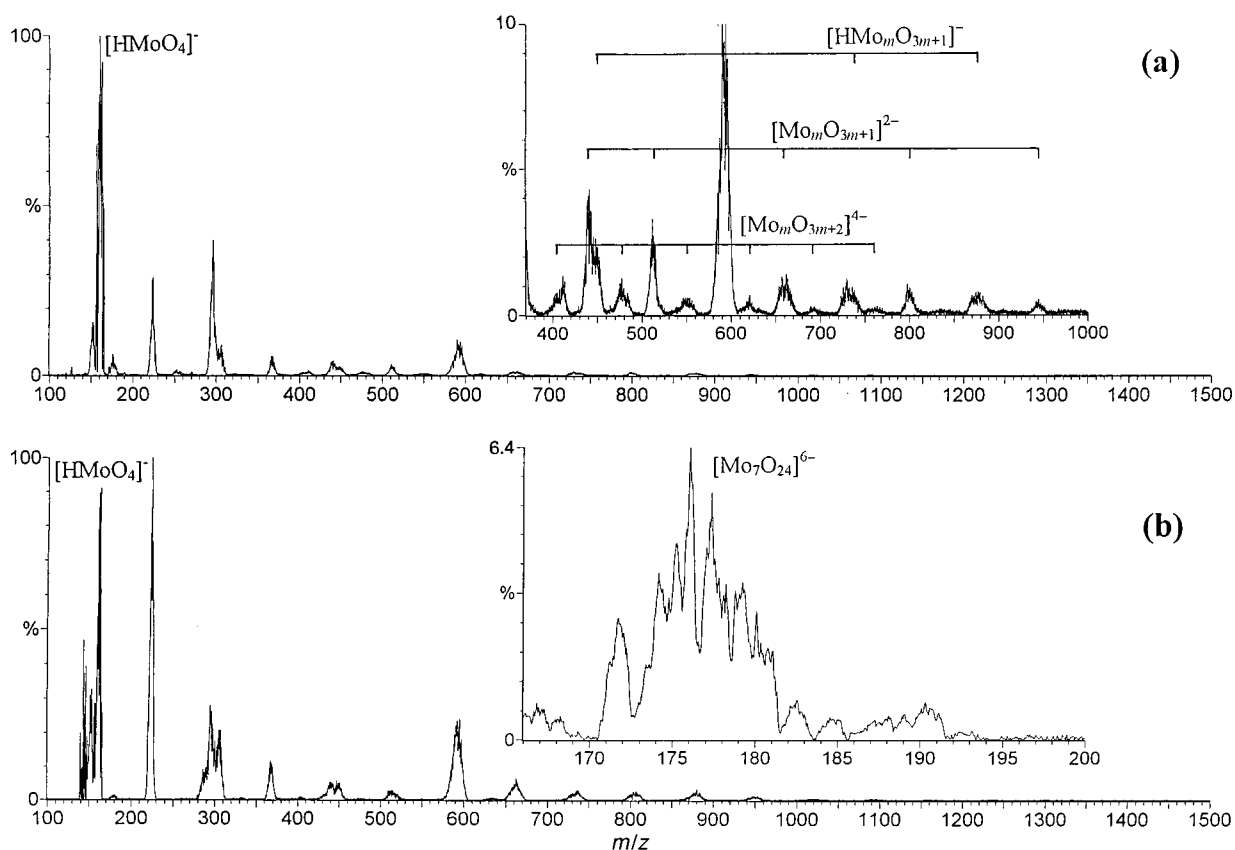

Fig. 2 Negative-ion ESMS of ammonium molybdate at pH 6.0: (a) CV set at -20 V; (b) CV set at -60 V.

$+20$ V. However, the lithium, sodium and potassium poly-oxomolybdate systems did show formation of aggregates at various pH and CV values. Figs. 4(a)–4(c) show the lithium, sodium and potassium molybdate mass spectra at pH 4.5 with CV $+60$ V. The isopolyoxomolybdate cations exhibit two series, $[Mo_mO_{4m}A_{2m+1}]^+$ and $[Mo_mO_{4m}A_{2m+2}]^{2+}$ (where $A = Li^+$, Na^+ or K^+ and m varies from 1 to 13). The doubly charged ions were observed only for m odd. Detailed assignments of the ESMS

data for pH 4.5 at CV $+20$ and $+60$ V are given in Table 3, with the results for pH 6.0 available as SUP 57467.

The above assignments are based purely on the m/z values of the peaks detected. Given the resolution of the instrument, it is possible that some minor peaks may overlap with peaks of the species listed above. Indeed, the product of a reductive proton-ation will have a similar mass to that of the parent species. It should be noted that no evidence of the reduced species

**Table 1** Negative-ion ESMS data of ammonium isopolyoxomolybdates

Ion observed	$(p,q)^a$	m/z Theoretical	pH 4.5		pH 6.0	
			CV = −20 V m/z exptl., %BPI	CV = −60 V m/z exptl., %BPI	CV = −20 V m/z exptl., %BPI	CV = −60 V m/z exptl., %BPI
$[MoO_3]^-$	—	143.9	—	145.2, 64.50	—	143.1, 46.99
$[Mo_mO_{3m+1}]$						
$[HMoO_4]^-$	1,1	160.9	162.2, 100	162.1, 100	160.1, 100	162.2, 91.02
$[Mo_2O_7]^{2-}$	2,2	151.9	151.8, 10.80	152.2, 8.66	152.1, 16.05	152.7, 32.77
$[HMo_2O_7]^-$	3,2	304.8	304.8, 6.81	306.0, 7.22	306.2, 9.35	305.2, 20.84
$[Mo_3O_{10}]^{2-}$	4,3	223.9	223.4, 17.51	233.7, 25.77	224.3, 29.00	224.0, 100
$[HMo_3O_{10}]^-$	5,3	448.8	448.7, 2.45	449.1, 2.45	450.2, 2.37	450.8, 5.20
$[Mo_4O_{13}]^{2-}$	6,4	295.9	295.8, 31.36	296.9, 14.45	296.2, 40.03	295.0, 28.18
$[HMo_4O_{13}]^-$	7,4	592.8	591.0, 9.73	592.6, 16.55	594.0, 10.17	591.8, 23.78
$[Mo_5O_{16}]^{2-}$	8,5	367.8	368.7, 2.85	367.7, 7.27	366.5, 5.81	367.2, 11.65
$[HMo_5O_{16}]^-$	9,5	736.7	730.6, 1.85	736.1, 4.59	735.7, 0.96	736.8, 3.03
$[Mo_6O_{19}]^{2-}$	10,6	439.8	440.7, 4.80	438.9, 4.32	440.9, 4.38	439.1, 5.34
$[HMo_6O_{19}]^-$	11,6	880.6	876.9, 1.11	877.8, 3.84	877.0, 0.81	880.1, 3.36
$[Mo_7O_{22}]^{2-}$	12,7	511.8	511.9, 3.83	510.4, 2.73	511.2, 3.36	513.1, 2.86
$[Mo_8O_{25}]^{2-}$	14,8	583.8	—	—	—	—
$[Mo_9O_{28}]^{2-}$	16,9	655.7	657.7, 1.58	655.2, 2.57	653.3, 1.01	662.2, 6.50
$[Mo_{10}O_{31}]^{2-}$	18,10	727.7	—	—	—	—
$[Mo_{11}O_{34}]^{2-}$	20,11	799.7	799.3, 1.46	799.9, 3.18	797.4, 1.06	803.2, 2.83
$[Mo_{12}O_{37}]^{2-}$	22,12	871.6	—	—	—	—
$[Mo_{13}O_{40}]^{2-}$	24,13	943.6	944.3, 0.68	943.8, 2.06	944.6, 0.53	946.8, 1.26
$[Mo_{14}O_{43}]^{2-}$	26,14	1015.6	1015.4, 0.54	1017.7, 1.25	1014.1, 0.35	1018.3, 0.65
$[Mo_{15}O_{46}]^{2-}$	28,15	1087.5	1085.7, 0.43	1088.3, 0.86	1090.5, 0.34	1088.3, 0.65
$[Mo_{16}O_{49}]^{2-}$	30,16	1159.5	1159.3, 0.20	1158.6, 0.87	—	1157.8, 0.49
$[Mo_{17}O_{52}]^{2-}$	32,17	1231.4	—	1233.7, 0.72	—	1232.7, 0.43
$[Mo_{18}O_{55}]^{2-}$	34,18	1303.4	—	1302.4, 0.71	—	1305.0, 0.41
$[Mo_{19}O_{58}]^{2-}$	36,19	1375.4	—	1376.3, 0.58	—	—
$[Mo_{20}O_{61}]^{2-}$	38,20	1447.4	—	1448.2, 0.52	—	—
$[Mo_mO_{3m+2}]$						
$[Mo_9O_{29}]^{4-}$	14,9	331.8	—	—	—	333.7, 0.67
$[Mo_{11}O_{35}]^{4-}$	18,11	403.8	404.8, 0.62	—	407.4, 0.92	404.0, 0.91
$[Mo_{13}O_{41}]^{4-}$	22,13	475.8	476.7, 0.84	—	476.9, 1.29	—
$[Mo_{15}O_{47}]^{4-}$	26,15	547.7	548.1, 0.90	—	548.4, 0.61	—
$[Mo_{17}O_{53}]^{4-}$	30,17	619.7	620.5, 0.63	—	620.6, 0.70	—
$[Mo_{19}O_{59}]^{4-}$	34,19	691.7	692.0, 0.47	—	692.5, 0.26	—
$[Mo_{21}O_{65}]^{4-}$	38,21	763.7	760.2, 0.46	—	761.1, 0.29	—
$[Mo_{23}O_{71}]^{4-}$	42,23	835.6	835.8, 0.38	—	—	—
$[Mo_mO_{3m+3}]$						
$[Mo_7O_{24}]^{6-}$	8,7	175.9	—	—	179.2, 1.44	176.0, 6.37

^{a} See eqn. (1).

$[MoO_3]^-$ was observed at CV −20 V, so that the data at this CV would not include such contributions. Thus much of the analysis described below will concentrate on the species and the observed percentage base peak intensity (%BPI) at this CV. Nevertheless, a more definitive analysis of the %BPI and/or the inferred structures of species (see below) with similar m/z ratios but different z values awaits a capillary electrophoresis MS-MS investigation. Finally, the formulae given in Tables 1–3 are symbolic and are not based on experimentally determined structures.

Discussion

The formation scheme for the possible polyoxomolybdate species can be represented by the general condensation or protonation reaction (1).[2,4,28] The observed species may or may not

$$pH^+ + q[MoO_4]^{2-} \rightleftharpoons [H_{p-2r}Mo_qO_{4q-r}]^{(2q-p)-} + rH_2O \quad (1)$$
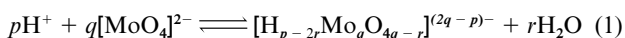
have the associated protons, but this will depend on the pH of the solution and the range of stability of the particular isopolyoxomolybdate. Equilibrium studies have shown that apart from

the protonated forms of the molybdate ion, that is $[HMoO_4]^-$ and H_2MoO_4, no species are observed until $[Mo_7O_{24}]^{6-}$, while to lower pH values $[HMo_7O_{24}]^{5-}$, β-$[Mo_8O_{26}]^{4-}$ and a more condensed species, perhaps related to the $[Mo_{36}O_{112}(H_2O)_{18}]^{8-}$ anion, are present.[19] Recent ^{95}Mo and ^{17}O studies have identified $[Mo_7O_{24}]^{6-}$, $[HMo_7O_{24}]^{5-}$, β-$[Mo_8O_{26}]^{4-}$ and the intermediate species $[H_3Mo_8O_{28}]^{5-}$ from pH 6 to 1.[42] Under the conditions employed in the present studies, however, the major species in the acidified molybdate solutions would have been $[Mo_7O_{24}]^{6-}$, as well as the protonated forms of the monomer. It is evident from the ESMS data presented above that considerable rearrangement has occurred, with the major species detected in all solutions being $[HMoO_4]^-$, while polymeric species larger than $[Mo_7O_{24}]^{6-}$ were present. This is a result of the extremely labile nature of these systems, which can undergo fast addition and/or loss of aggregation units. In general, less labile systems remain intact and only undergo limited dehydration and related reactions during passage through the gas phase, over a range of cone voltages.[43]

As noted above, in bulk investigations, the $[Mo_7O_{24}]^{6-}$ ion is the dominant polymeric species in the solutions employed. Hence it would be anticipated that, as ESMS is a "soft" ionization technique, this species should be dominant at the pH
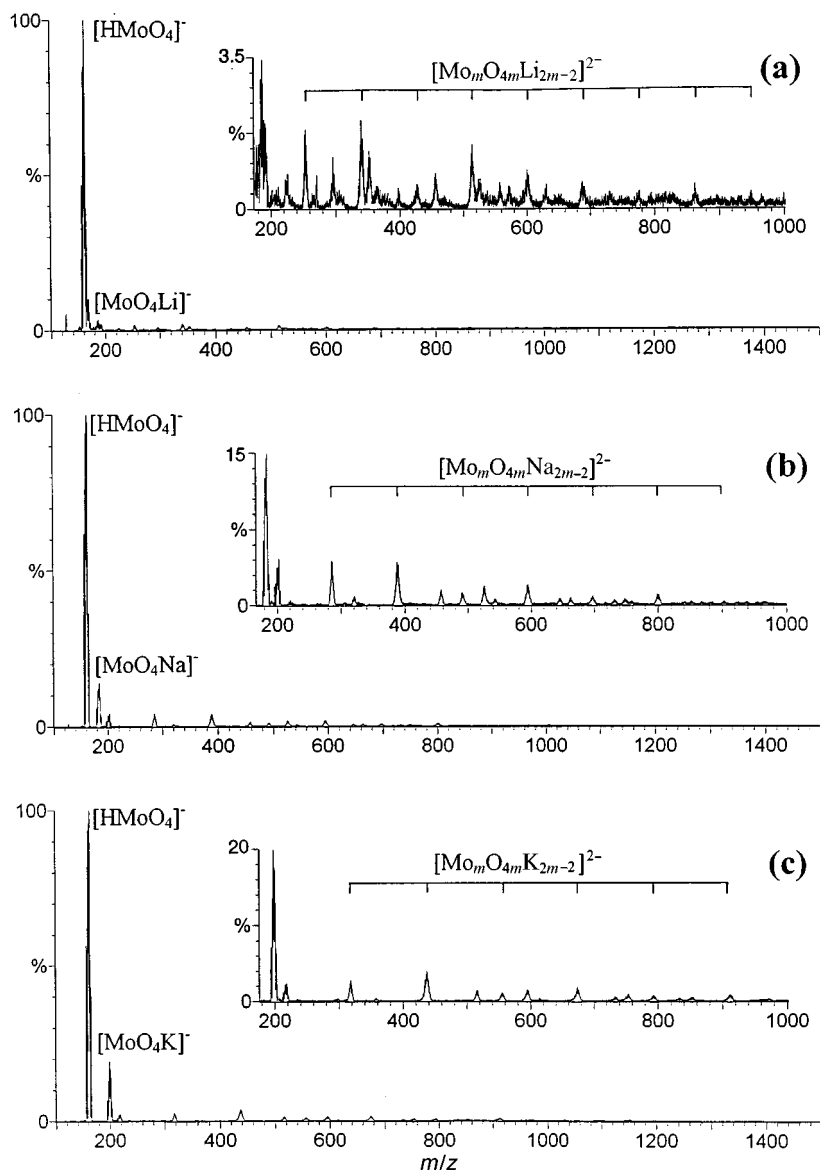
Fig. 3 Negative-ion ESMS of alkali metal molybdate at pH 4.5 and CV set at -20 V: (a) lithium; (b) sodium; (c) potassium system.

values examined. It is present at pH 6.0 and at both CV -20 and -60 V, but with a low %BPI. At pH 4.5 it is not detected at either CV value. Thus the large abundance of $[HMoO_4]^-$ in all of the ESMS spectra of the ammonium and alkali metal molybdate systems suggests that the $[Mo_7O_{24}]^{6-}$ ion dissociates according to eqn. (2). This cannot have proceeded to

$$[Mo_7O_{24}]^{6-} + 4H_2O \rightleftharpoons 7[HMoO_4]^- + H^+ \qquad (2)$$
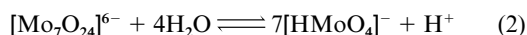
completion as the presence of this species is required as a precursor to the formation of the $[Mo_mO_{3m+2}]^{4-}$ series of anions, as shown below.

It is known from bulk kinetic studies that concentration terms for $[HMoO_4]^-$ appear in the rate laws for both the assembly and dissociation of (hetero)polyoxomolybdate anion frameworks.[40,41] Therefore, copious quantities of $[HMoO_4]^-$ in the charged droplets provide a source of $\{MoO_3\}$ aggregation units *via* eqn. (3) for the assembly of polymeric species in

$$[HMoO_4]^- + \{H^+\} \rightleftharpoons \{MoO_3\} + H_2O \qquad (3)$$
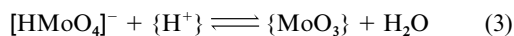
aqueous solution, which gives rise to the large range of aggregates observed in all series in the present studies, many with

$m > 7$. Here $\{H^+\}$ represents a protonation site on an isopoly-oxomolybdate anion suitable for addition of $\{MoO_3\}$ by the $[HMoO_4]^-$ ion with elimination of a water molecule. Thus, the ESMS technique should provide valuable insights into the polymerization reactions of isopoly- and heteropoly-oxo-metalates and their intermediate fragments.

1 The nature of protonated $[MoO_4]^{2-}$ in solution

The formation of polyoxomolybdates in the bulk (*e.g.* $[Mo_7O_{24}]^{6-}$) is a rapid reaction and requires an expansion of the co-ordination number of molybdenum(VI) from 4 to 6. It is assumed that monoprotonation of $[MoO_4]^{2-}$ also enables this reaction to occur. However, the (%BPI, m/z ratio) of (tetra-hedral) $[HMoO_4]^-$ and (octahedral) $[MoO(OH)_5]^-$ {or an alternative form such as $[MoO_3(OH)(H_2O)_2]^-$} are (100%, 162) and (0%, 197) respectively. On the basis of the mass peaks measured in this investigation, monoprotonated monomoly-bdate is of the form $[HMoO_4]^-$ {or better $[MoO_3(OH)]^-$} and not as $[MoO(OH)_5]^-$. Nevertheless, it should be noted that the ESMS results could be also consistent with $[MoO(OH)_5]^-$ rapidly dissociating into $[HMoO_4]^-$ through the process (4) where A is the inert collision medium such as nitrogen. Such a process may readily occur because of the lability of these systems.

Table 2   Negative-ion ESMS data of alkali metal polyoxomolybdates (pH 4.5)

| Ion observed	A = Lithium			Sodium			Potassium		
	m/z Theoretical	CV = −20 V m/z exptl., %BPI	CV = −60 V m/z exptl., %BPI	m/z Theoretical	CV = −20 V m/z exptl., %BPI	CV = −60 V m/z exptl., %BPI	m/z Theoretical	CV = −20 V m/z exptl., %BPI	CV = −60 V m/z exptl., %BPI
$[MoO_3]^-$	143.9	—	145.2, 53.06	143.9	—	145.3, 41.22	143.9	—	145.5, 45.82
$[AMo_mO_{3m+1}]^-$									
$[HMoO_4]^-$	160.9	162.5, 100	162.4, 100	160.9	162.5, 100	161.1, 100	160.9	162.5, 100	160.2, 100
$[AMoO_4]^-$	166.9	168.2, 10.25	166.1, 21.04	182.9	184.2, 14.42	184.2, 13.41	198.9	198.1, 19.19	200.8, 25.41
$[AMo_2O_7]^-$	310.9	—	309.1, 0.91	326.9	—	—	342.9	—	—
$[AMo_3O_{10}]^-$	454.8	456.4, 0.83	454.8, 0.59	470.8	—	—	486.8	—	—
$[AMo_4O_{13}]^-$	598.7	600.2, 0.91	601.0, 1.52	614.7	—	—	630.8	—	—
$[AMo_5O_{16}]^-$	742.7	—	746.9, 0.56	758.7	—	—	774.7	—	—
$[Mo_mO_{4m}A_{2m-2}]^{2-}$									
$[Mo_3O_{12}A_4]^{2-}$	253.9	253.6, 1.85	—	285.9	285.2, 4.21	285.0, 0.18	317.9	318.3, 2.65	—
$[Mo_4O_{16}A_6]^{2-}$	340.8	340.0, 2.05	340.9, 7.58	388.9	387.9, 4.13	388.8, 7.36	436.9	436.7, 3.83	436.5, 6.68
$[Mo_5O_{20}A_8]^{2-}$	427.8	426.6, 0.57	427.7, 0.26	491.9	491.5, 1.19	492.4, 0.27	555.8	556.3, 1.06	—
$[Mo_6O_{24}A_{10}]^{2-}$	514.8	514.6, 1.49	512.2, 1.95	594.8	595.0, 1.91	594.9, 2.20	674.8	674.0, 1.82	672.9, 1.45
$[Mo_7O_{28}A_{12}]^{2-}$	601.8	600.2, 0.62	601.0, 1.52	697.8	697.9, 0.87	697.2, 0.76	793.8	793.6, 0.84	794.5, 0.26
$[Mo_8O_{32}A_{14}]^{2-}$	688.8	687.3, 0.62	688.0, 2.49	800.8	798.7, 0.90	801.2, 2.07	912.8	912.3, 0.89	911.8, 1.58
$[Mo_9O_{36}A_{16}]^{2-}$	775.7	775.9, 0.40	774.8, 0.84	903.8	902.3, 0.34	903.4, 0.73	1031.7	1030.5, 0.45	1031.9, 0.68
$[Mo_{10}O_{40}A_{18}]^{2-}$	862.7	862.0, 0.56	863.8, 1.55	1006.7	1005.2, 0.57	1008.1, 1.36	1150.7	1151.2, 0.49	1149.3, 1.31
$[Mo_{11}O_{44}A_{20}]^{2-}$	949.7	949.5, 0.40	949.3, 0.91	1109.7	1109.8, 0.31	1109.3, 0.72	1269.7	—	1269.7, 0.60
$[Mo_{12}O_{48}A_{22}]^{2-}$	1036.6	1036.1, 0.31	1035.6, 1.12	1212.6	1211.0, 0.31	1211.1, 0.85	1388.6	1385.5, 0.25	1388.7, 0.94
$[Mo_{13}O_{52}A_{24}]^{2-}$	1123.6	1122.3, 0.27	1120.9, 0.65	1315.6	1313.9, 0.21	1314.2, 0.45	1508.8	—	—
$[Mo_{14}O_{56}A_{26}]^{2-}$	1210.6	1208.9, 0.20	1210.4, 0.67	1418.6	1418.0, 0.20	1416.4, 0.51	1627.8	—	—
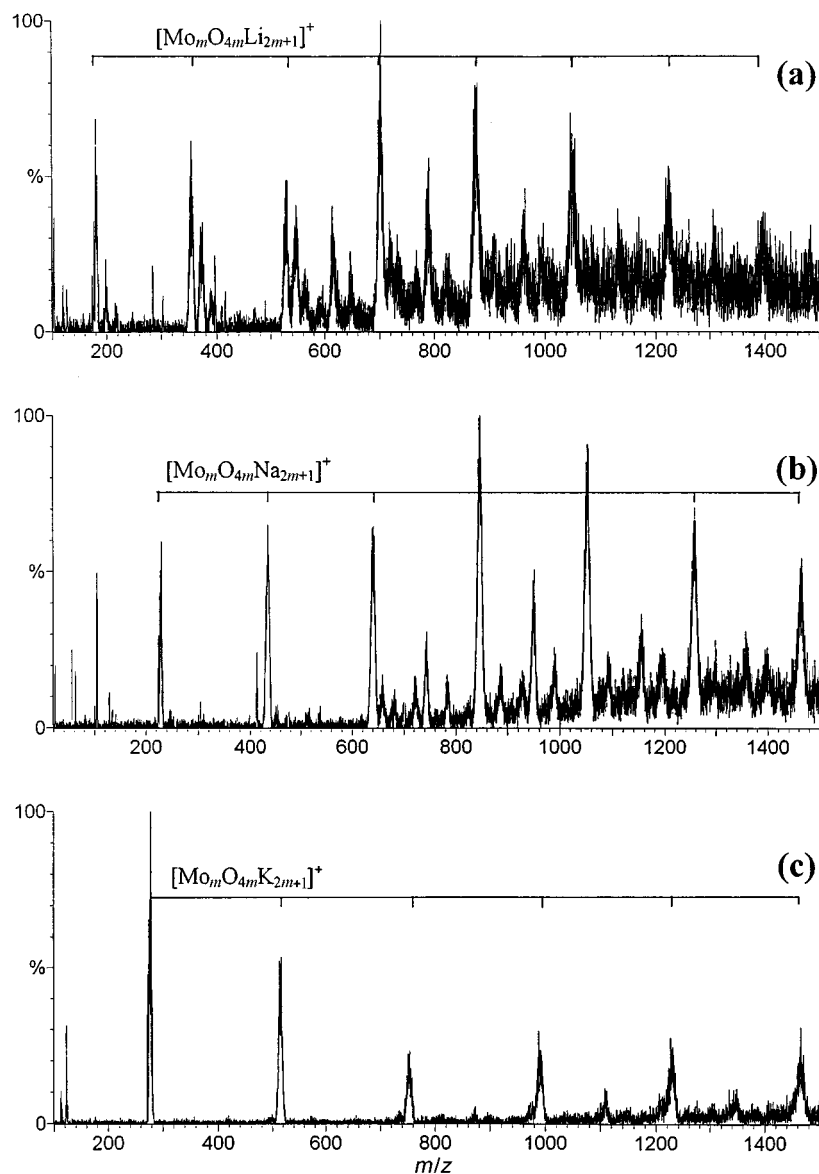
Fig. 4 Positive-ion ESMS of alkali metal molybdate at pH 4.5 and CV set at +60 V: (a) lithium; (b) sodium; (c) potassium system.
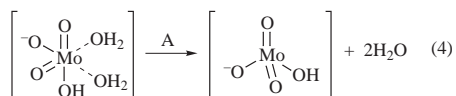
2 The ammonium molybdate systems

The $[HMo_mO_{3m+1}]^-$ and $[Mo_mO_{3m+1}]^{2-}$ series. The two series, $[HMo_mO_{3m+1}]^-$ and $[Mo_mO_{3m+1}]^{2-}$, were found in studies of the ammonium molybdate system. The former was observed from $m = 1$ to 6 and the second from $m = 2$ to 20. The recent investigation of Siu and co-workers[37] of the three tetrabutyl-ammonium salts of $[Mo_2O_7]^{2-}$, $[Mo_6O_{19}]^{2-}$ and $[Mo_8O_{26}]^{4-}$ in aqueous–organic solvents identified the parent ion as the base peak for each solution. Other anions, such as $[Mo_3O_{10}]^{2-}$, $[Mo_4O_{13}]^{2-}$ and $[Mo_5O_{16}]^{2-}$, all members of the $[Mo_mO_{3m+1}]^{2-}$ series, were regarded as fragment ions due to the multiple removal of formal $\{MoO_3\}$ units from precursor ions. The fragment ions observed had relative %BPI values ranging from 0.1 to 19%. Additionally, the quadruply charged species, $[Mo_6O_{20}]^{4-}$ (which has a similar m/z to $[Mo_3O_{10}]^{2-}$), was likewise regarded as a fragment ion of the precursor species $[Mo_8O_{26}]^{4-}$. Both types of species (doubly and quadruply charged ions) that were detected have also been observed in this investigation. However, the presence of protonated

forms of several of these polyoxomolybdate ions such as the $[HMo_mO_{3m+1}]^-$ series, as well as $[HMoO_4]^-$ ($m = 1$), were not reported. The latter is the most abundant peak in nearly all of the spectra measured in this investigation, while no species with an aggregation greater than an octamolybdate were reported in the study by Lau *et al.*[37]

It should be noted that the evaporation process in ESMS can have significant chemical effects. The removal of ammonia (as is evident from our ESMS data of the ammonium molybdate systems) results in a rapidly changing pH of the charged droplets. Thus protonated forms ($[HMo_mO_{3m+1}]^-$) of the early members of the $[Mo_mO_{3m+1}]^{2-}$ series are observed, but terminate at $m = 6$. As the Lewis basicity of the anions rapidly diminishes with increasing polymerization the latter members of this series ($m > 6$) remain unprotonated.

For the $[Mo_mO_{3m+1}]^{2-}$ series, the peak at m/z 296 in Table 1 can be assigned as either the $[Mo_4O_{13}]^{2-}$ or $[Mo_8O_{26}]^{4-}$ anion. It is possible to distinguish between these species by comparing their calculated line shapes with the experimental data. Fig. 5(a) shows the experimental spectrum of the peak at m/z 296, whereas Fig. 5(b) and 5(c) show the theoretical spectra line shapes of the $[Mo_4O_{13}]^{2-}$ and $[Mo_8O_{26}]^{4-}$ anions respectively. The ratios of the full width at half-maximum height (FWHM) of the theoretical spectral peaks *versus* experiment for the $[Mo_4O_{13}]^{2-}$ and $[Mo_8O_{26}]^{4-}$ ions are 0.98 and

Table 3   Positive-ion ESMS data of alkali metal polyoxomolybdates (pH 4.5)

Ion observed	A = Lithium			Sodium			Potassium		
	m/z Theoretical	CV = +20 V m/z exptl., %BPI	CV = +60 V m/z exptl., % BPI	m/z Theoretical	CV = +20 V m/z exptl., %BPI	CV = +60 V m/z exptl., %BPI	m/z Theoretical	CV = +20 V m/z exptl., %BPI	CV = +60V m/z exptl.,%BPI
$[Mo_mO_{4m}A_{2m+1}]^+$									
$[MoO_4A_3]^+$	180.9	—	179.9, 68.48	228.9	229.8, 0.99	229.9, 59.68	276.9	278.0, 37.09	278.0, 35.84
$[Mo_2O_8A_5]^+$	354.9	—	354.8, 61.41	434.9	434.5, 0.63	434.9, 64.98	514.9	514.9, 46.44	514.8, 21.48
$[Mo_3O_{12}A_7]^+$	528.8	—	528.3, 48.70	640.8	641.0, 0.65	641.1, 64.51	752.8	754.1, 18.72	752.2, 7.49
$[Mo_4O_{16}A_9]^+$	702.8	—	703.1, 100	846.8	845.9, 1.04	846.5, 100	990.8	989.4, 16.75	990.9, 10.80
$[Mo_5O_{20}A_{11}]^+$	876.7	—	878.4, 80.09	1052.7	1052.3, 0.86	1051.4, 90.81	1228.7	1227.9, 7.39	1227.8, 12.59
$[Mo_6O_{24}A_{13}]^+$	1050.6	—	1046.5, 70.28	1258.6	1258.6, 0.69	1257.0, 70.54	1466.6	1456.6, 6.88	1464.4, 13.13
$[Mo_7O_{28}A_{15}]^+$	1224.6	—	1222.3, 53.16	1464.6	1461.2, 0.56	1463.9, 54.41	1704.6	—	1702.2, 11.26
$[Mo_mO_{4m}A_{2m+2}]^{2+}$									
$[Mo_3O_{12}A_8]^{2+}$	267.7	—	—	331.9	—	—	395.9	396.0, 16.91	—
$[Mo_5O_{20}A_{12}]^{2+}$	441.5	—	—	537.8	—	—	633.8	634.6, 19.52	—
$[Mo_7O_{28}A_{16}]^{2+}$	647.8	—	648.2, 21.18	743.8	742.9, 0.76	744.1, 30.84	871.8	871.2, 10.98	872.1, 1.99
$[Mo_9O_{36}A_{20}]^{2+}$	789.7	—	789.1, 51.00	949.7	949.7, 0.68	948.1, 45.61	1109.7	1109.7, 10.29	1110.0, 6.07
$[Mo_{11}O_{44}A_{24}]^{2+}$	963.7	—	964.3, 47.60	1155.7	—	1154.5, 36.55	1347.7	—	1348.2, 4.17
$[Mo_{13}O_{52}A_{28}]^{2+}$	1136.8	—	—	1361.6	—	1356.8, 30.95	1585.6	—	1582.0, 5.74

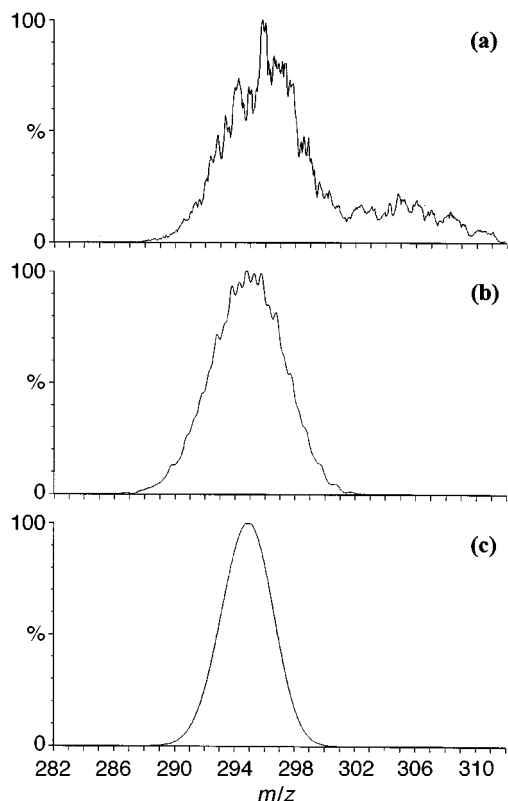**Fig. 5** Comparison of negative-ion ESMS line shapes: (a) experimental line shape of $[Mo_4O_{13}]^{2-}$; (b) calculated line shape of $[Mo_4O_{13}]^{2-}$ (with FWHM = 0.8 Dalton and isotope separation = 1.0 Dalton); (c) calculated line shape of $[Mo_8O_{26}]^{4-}$ (with FWHM = 0.8 Dalton and isotope separation = 1.0 Dalton).

Fig. 6 Possible structures for: (a) $[Mo_mO_{3m+1}]^{2-}$, $[T^c]_i$ for $i = 2$, 4 or 16; (b) $[Mo_mO_{3m+1}]^{2-}$, $[(T^cO^e)_i]T^e$ for $i = 1$, 3 or 7; (c) $[Mo_mO_{4m-}A_{2m-2}]^{2-}$, $[(O^e)_i]T^e$ for $i = 2$–4.

0.70 : 1 respectively. Hence, the ESMS datum is more consistent with the assignment of this peak to the $[Mo_4O_{13}]^{2-}$ species. This is also the case for all assigned doubly charged ions.

Table 1 shows that the %BPI of $[Mo_4O_{13}]^{2-}$ at pH 4.5 and 6.0 with CV −20 V are 31 and 40% respectively. At CV −60 V the %BPI are reduced to 14 and 28% respectively. This indicates that fragmentation of this species has occurred at the higher CV. This is consistent with the concomitant relative increases in the %BPI values of $[Mo_3O_{10}]^{2-}$ and $[Mo_5O_{16}]^{2-}$, which are produced *via* the dissociation reaction (5). Thus the following

$$2[Mo_mO_{3m+1}]^{2-} \longrightarrow [Mo_{m-1}O_{3m-2}]^{2-}$$
$$+ [Mo_{m+1}O_{3m+4}]^{2-} \quad (5)$$
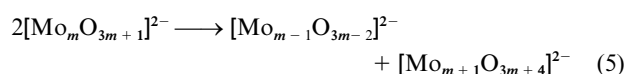
analysis will center on the spectra measured at CV −20 V, which are not subject to such fragmentation reactions.

Addition polymerization. The open-chain polymerization or aggregation of the isopolyoxomolybdate systems may occur either by edge or corner sharing of the oxygen atoms. There are other possible combinations, but these are less likely. It should be noted that the polymerization or aggregation may not be associated with the ions in bulk solution due to the ESMS process, which dries charged droplets in the production of the charged molecular aggregates. This is especially important for these labile systems, where water molecules that may have initially occupied axial positions in molybdate octahedra are removed, leaving a tetrahedral residue [eqn. (4)].

To assist in the interpretation of the mass spectra of the $[Mo_mO_{3m+1}]^{2-}$ series, investigation of the %BPI values of the members is informative. In an addition polymerization mechanism, once the "seed" has been constructed, polymerization is driven by the addition of a monomer or moiety for the "growth" of the chain. The degree of polymerization, q, is given
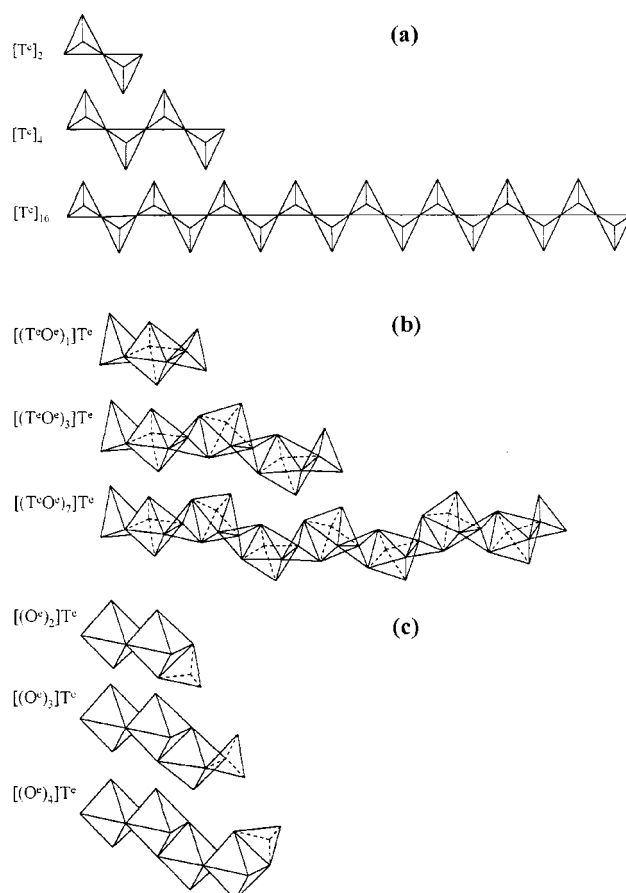
by N_0/N_t (where N_0 is the number of molybdate monomers available for addition at time zero and N_t is the number available at time t), and must be proportional to the quantity of polymers present, that is to the %BPI. Hence $\ln q \approx p \propto -m$, where m is the number of molybdate units in the polymer chain and p is the extent of the reaction, $(N_0 − N_t)/N_0$. Therefore a plot of the logarithm of the %BPI *versus* the number of molybdate units in the aggregates should reveal a straight line with a negative slope. Such a correlation is observed with the correlation coefficients for m (odd, even, total) being (0.8933, 0.9081, 0.8945) respectively. This suggests that the assembly of these aggregates in this series is *via* an addition polymerization mechanism.

Inferred structures. To characterize the ESMS aggregates detected in this investigation the following classification will be invoked. In the case of the ammonium molybdate system members of the $[Mo_mO_{3m+1}]^{2-}$ series (and related protonated forms) were observed. Two different formulae can be invoked to depict the inferred structures and molybdenum valencies of the species. Aggregates with even or odd molybdate units may have a structural formula denoted as $[T^c]_i$, where the square brackets enclose the "i" repeating tetrahedral unit "T", and the superscript "c" indicates that corner oxygens are shared. It should be noted that "i" must equal m. For example, the largest aggregate observed at CV −20 V and pH 4.5 is $[Mo_{16}O_{49}]^{2-}$, which is denoted as $[T^c]_{16}$. In the corner-shared tetrahedral structure the $\{MoO_3\}$ moiety is the additive unit for the polymerization process, generated from the presence of $[HMoO_4]^-$ [see eqn. (3)]. The polymerization process may involve corner-shared octahedral structures which are desolvated via eqn. (4) during the ESMS process, leaving tetrahedral residues. Nevertheless, the analytes detected do not exhibit the presence of co-ordinated water ligands. Fig. 6(a) gives a schematic of possible

structures for three members of the series. Also, it should be noted that closed-packed structures are generally associated with larger-sized highly negatively charged aggregates [16,31,44] and are not applicable nor consistent with the O : Mo ratios observed in the ESMS spectra for this series.

There is experimental evidence, according to crystallographic studies of isopolyoxomolybdates,[16,31,44] of a repeating unit of the form $[(O^eT^c)_i]$, where MoO_6 octahedra (denoted as "O") share corners with MoO_4 tetrahedra and with the adjacent MoO_6 octahedra in the chain as exemplified by $([Mo_2O_7]^{2-})_\infty$ in $[NH_4]_2[Mo_2O_7]$. The gas-phase ESMS data do not support these alternating structures. For example, for a 5-molybdate fragment derived from the infinite chain $([Mo_2O_7]^{2-})_\infty$ in $[NH_4]_2$-$[Mo_2O_7]$ there are several fragments that may occur in the gas phase. The least-charged fragments have the mass formulae $[Mo_5O_{19}]^{8-}$ and $[Mo_5O_{20}]^{10-}$, but neither is observed in the negative-ion ESMS spectra.

The ESMS data for m odd are also consistent with the structural formula $[(T^eO^e)_i]T^e$, with i now being equal to $(m-1)/2$, and the superscript "e" implying that the oxygens are now edge shared, with the four oxygens in the non-terminating tetrahedral units exhibiting partial double bonding to molybdenum. The "T" outside of the square bracket is a terminating tetrahedral residue. The largest polymer observed at CV −20 V and pH 4.5 is for $m = 15$, which yields a structural formula of $[(T^eO^e)_7]T^e$ corresponding to $[Mo_{15}O_{46}]^{2-}$. Fig. 6(b) gives a schematic of these structures with m odd for three members of the series.

To assist in delineating which structures may be appropriate for the $[Mo_mO_{3m+1}]^{2-}$ series, an analysis of the correlation coefficients from the addition polymerization analysis is informative. As each component correlation coefficient is similar to the overall value there appears to be no reason to assume that a different assembly mechanism should occur for m even or odd. In the absence of more definitive experimental evidence, the corner-shared tetrahedral structure representation, $[T^c]_i$, with the $\{MoO_3\}$ moiety being the additive unit, appears to be a more consistent interpretation of the ESMS data.

The $[Mo_mO_{3m+2}]^{4-}$ series. The species of the series $[Mo_mO_{3m+2}]^{4-}$ are highly charged and so would be expected to have closed-packed structures. In fact, the structure of $[Mo_8O_{26}]^{4-}$ has been established crystallographically, and consists of eight MoO_6 octahedra sharing edges (*i.e.* $[O^e]_8$).[16,31,44] The $[Mo_7O_{24}]^{6-}$ ion appears to be the likely seed for the $[Mo_mO_{3m+2}]^{4-}$ series, since the series begins with $m > 7$, and the addition of a formal $\{MoO_2^{2+}\}$ unit together with $\{MoO_3\}$ would yield the first member of the series. The $\{MoO_2^{2+}\}$ unit can be generated from $[HMoO_4]^-$ *via* eqn. (6). The $[Mo_9O_{29}]^{4-}$

$$[HMoO_4]^- + 3\{H^+\} \rightleftharpoons \{MoO_2^{2+}\} + 2H_2O \quad (6)$$
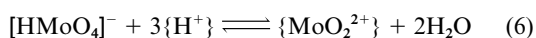
structure may be simply generated by the addition of $\{MoO_2^{2+}\}$ and $\{MoO_3\}$ aggregation units in adjacent sites on an $[Mo_7O_{24}]^{6-}$ ion, such that the $\{MoO_2^{2+}\}$ unit shares four oxygen sites and the $\{MoO_3\}$ unit three sites on the seed. Further additions of $\{MoO_3\}$ units occur on edge-sharing positions of available MoO_6 octahedra, thereby generating this series. Alternatively, the source of the additive $\{MoO_2^{2+}\}$ and $\{MoO_3\}$ units may be the $[HMo_2O_7]^-$ ion, which is present with a reasonably large %BPI (see Table 1) for CV −20 V at pH 4.5 and 6 *via* eqn. (7).

$$[HMo_2O_7]^- + 3\{H^+\} \rightleftharpoons \{MoO_2^{2+}\} + \{MoO_3\} + 2H_2O \quad (7)$$
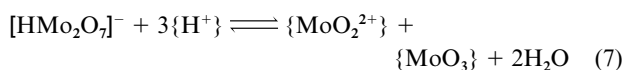
The structure of the $[Mo_7O_{24}]^{6-}$ ion is well known, and consists of seven MoO_6 octahedra sharing edges (*i.e.* $[O^e]_7$).[16,31,44] At pH 6.0 there is an approximate fourfold increase in the %BPI of this species between CV −20 and −60 V, which

suggests that the increase is due to fragmentation *via* the dissociation reaction (8) where $m = 9$. However, the low %BPI

$$2[Mo_mO_{3m+2}]^{4-} \longrightarrow [Mo_{m-2}O_{3m-3}]^{6-} + [Mo_{m+2}O_{3m+7}]^{2-} \quad (8)$$
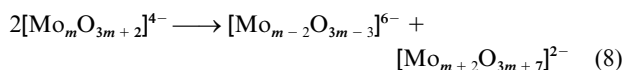
for the $[Mo_7O_{24}]^{6-}$ ion has been attributed to the generation of $[HMoO_4]^-$ [see eqn. (2)]. Nevertheless, the absence of other members of a $[Mo_mO_{3m+3}]^{6-}$ series suggests that even if small quantities of the $[Mo_7O_{24}]^{6-}$ ion are present it may act as a seed to generate larger sized polymers.
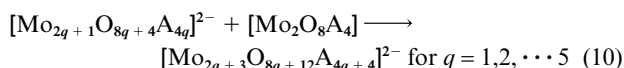
The rapid dissociation reaction (9) where m is even ensures a low %BPI of these even-membered species when compared with the m odd ions. Nevertheless, within the resolution of the instrument, the m/z overlap of the $[Mo_mO_{3m+2}]^{4-}$ and $[Mo_mO_{3m+1}]^{2-}$ (for m even) precludes a definitive analysis as to the extent of dissociation according to eqn. (9).
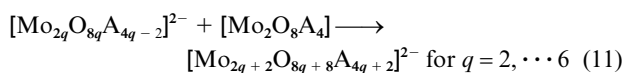
$$2[Mo_mO_{3m+2}]^{4-} \longrightarrow [Mo_{m-1}O_{3m-1}]^{4-} + [Mo_{m+1}O_{3m+5}]^{4-} \quad (9)$$
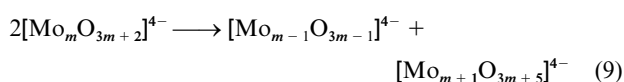
3 The alkali metal molybdate systems

The $[Mo_mO_{3m+1}A]^-$ and $[Mo_mO_{4m}A_{2m-2}]^{2-}$ series. The alkali metal molybdate solutions yield two sequences in negative-ion mode due to the incorporation of the alkali metal cations. The $[Mo_mO_{3m+1}A]^-$ series is similar in structure to that observed in the ammonium molybdate system except for the addition of an alkali metal cation. The series is severely truncated in the sodium and potassium systems and, because of the lack of data, no attempt was made to apply the addition polymerization model. There is no evidence for a series related to the more highly charged series found in the ammonium molybdate system.

The second series observed has the general formula $[Mo_mO_{4m}A_{2m-2}]^{2-}$. Plots of the logarithm of the %BPI for the $[Mo_mO_{4m}A_{2m-2}]^{2-}$ series *versus* the number of molybdate units (m) in the aggregates yield correlation coefficients for the lithium, sodium and potassium systems for m (odd, even, total) of (0.8049, 0.9744, 0.8284), (0.9221, 0.9890, 0.9083) and (0.9512, 0.9985, 0.8783) respectively. There are significant differences between the component correlation coefficients and the overall correlation, which suggests that the addition polymerization begins from different seeds. For example, starting with an odd-seed the addition polymerization sequence is (10) whereas

$$[Mo_{2q+1}O_{8q+4}A_{4q}]^{2-} + [Mo_2O_8A_4] \longrightarrow [Mo_{2q+3}O_{8q+12}A_{4q+4}]^{2-} \text{ for } q = 1,2,\cdots 5 \quad (10)$$

starting with an even-seed the addition polymerization sequence is (11). An additive $[Mo_2O_8A_4]$ moiety for both the even and

$$[Mo_{2q}O_{8q}A_{4q-2}]^{2-} + [Mo_2O_8A_4] \longrightarrow [Mo_{2q+2}O_{8q+8}A_{4q+2}]^{2-} \text{ for } q = 2,\cdots 6 \quad (11)$$
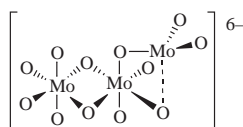
odd seeds is therefore consistent with the component correlation coefficients for odd and even sequences being better correlated than for the total correlation.

The open-chained structures for both odd and even m can be designated as $[(O^e)_i]T^e$, where $i = m - 1$. For example, in all cases, aggregation first occurs for $i = 2$ which corresponds to the $[Mo_3O_{12}A_4]^{2-}$ ion for each alkali metal system. The tetrahedral unit may have had initially two axial water molecules which were desolvated during the drying process *via* eqn. (4). Fig. 6(c) depicts three members of the sequence. On electrostatic grounds the negatively charged oxygen ligands would distort the octahedral shape (which is not shown in this schematic). Moreover, the structures have been drawn exhibiting *cis*-dioxo MoO_2 units which are consistent with this structural feature as

found in the known structures of isopolymolybdates.[2] The ESMS data are also supportive of structures in which the tetrahedral unit occupies positions other than the terminal position, although this would not lead to a facile polymer condensation mechanism.

The additive unit described above, $[Mo_2O_8A_4]$, must be dimeric and not two monomeric $A_2[MoO_4]$ units since the addition of the latter is inconsistent with the correlations observed in this work. The additive unit structure is therefore designated as (O^eT) which supports the polymerization process suggested by Kepert.[45] The addition polymerization process given by eqns. (10) and (11) suggests that the tetrahedral residue is in the terminal position since the terminal oxygens are perpendicular to the plane of the adjoining octahedra and the insertion of the octahedral residue of the additive $[Mo_2O_8A_4]$ moiety would sweep these oxygen atoms into axial positions as required by the $[(O^e)_i]T^e$ structural respresentation.

The $[Mo_mO_{4m}A_{2m+1}]^+$ and $[Mo_mO_{4m}A_{2m+2}]^{2+}$ series. The positive-ion ESMS data for the singly charged cations are consistent with the structural formula of the anions, *i.e.* $[(O^e)_i]T^e$, where $i = m - 1$, with the open-chain interleaved by the alkali metal cations, stabilizing the negatively charged oxygens. For the sodium and potassium systems the doubly charged cations have the same structural formula as the anions except that there is an additional alkali metal cation in the structure. A schematic of a singly charged $[Mo_3O_{12}K_7]^+$ and doubly charged $[Mo_3O_{12}K_8]^{2+}$ may be represented as shown below. For simplifi-

cation the alkali metal cations have been omitted. They most likely occupy edge-bridging or face-capping positions on the individual MoO_6 octahedra.

Acknowledgements

References

1 C. L. Hill, *Chem. Rev.*, 1998, **98**, 1.
2 M. T. Pope, *Inorganic Chemistry Concepts 8, Heteropoly and Isopoly Oxometalates*, Springer, Berlin, 1983.
3 K. F. Jahr and J. Fuchs, *Angew. Chem., Int. Ed. Engl.*, 1966, **5**, 689.
4 K. H. Tytko and O. Glemser, *Adv. Inorg. Chem. Radiochem.*, 1976, **19**, 239.
5 H. T. Evans, Jr., *Perspect. Struct. Chem.*, 1971, **4**, 2.
6 E. Darmois and J. Périn, *C. R. Acad. Sci.*, 1923, **177**, 762.
7 Y. Doucet and S. Bugnon, *J. Chim. Phys.*, 1957, **54**, 155.
8 E. Richardson, *J. Inorg. Nucl. Chem.*, 1959, **9**, 267.
9 C. Heitner-Wirguin and R. Cohen, *J. Inorg. Nucl. Chem.*, 1964, **26**, 161.
10 D. S. Honig and K. Kustin, *Inorg. Chem.*, 1972, **11**, 65.
11 N. Kiba and T. Takeuchi, *J. Inorg. Nucl. Chem.*, 1974, **36**, 847.
12 K. Y. S. Ng and E. Gulary, *Polyhedron*, 1984, **3**, 1001.
13 K. H. Tytko, G. Baethe and J. J. Cruywagen, *Inorg. Chem.*, 1985, **24**, 3132.
14 T. Ozeki, H. Kihara and S. Ikeda, *Anal. Chem.*, 1988, **60**, 2055.
15 S. Himeno, H. Niiya and T. Ueda, *Bull. Chem. Soc. Jpn.*, 1997, **70**, 631.
16 I. Lindqvist, *Ark. Kemi*, 1950, **2**, 349.
17 G. Schwarzenbach and J. Meier, *J. Inorg. Nucl. Chem.*, 1958, **8**, 302.
18 R. H. Busey and O. L. Keller, *J. Chem. Phys.*, 1964, **41**, 215.
19 Y. Sasaki and L. G. Sillén, *Acta Chem. Scand.*, 1964, **18**, 1014.
20 E. F. C. H. Rohwer and J. J. Cruywagen, *J. S. Afr. Chem. Inst.*, 1963, **16**, 26.
21 J. Aveston, E. W. Anacker and J. S. Johnson, *Inorg. Chem.*, 1964, **3**, 735.
22 E. F. C. H. Rohwer and J. J. Cruywagen, *J. S. Afr. Chem. Inst.*, 1964, **17**, 145.
23 D. V. S. Jain, *Indian J. Chem.*, 1970, **8**, 945.
24 G. Wiese and D. Böse, *Z. Naturforsch., Teil B*, 1972, **27**, 897.
25 I. Knöpnadel, H. Hartl, W.-D. Hunnius and J. Fuchs, *Angew. Chem., Int. Ed. Engl.*, 1974, **13**, 823.
26 A. W. Armour, M. G. B. Drew and P. C. H. Mitchell, *J. Chem. Soc. Dalton Trans.*, 1975, 1493.
27 V. W. Day, M. F. Fredrich, W. G. Klemperer and W. Shum, *J. Am. Chem. Soc.*, 1977, **99**, 6146.
28 M. K. Cooper and J. E. Salmon, *J. Chem. Soc.*, 1962, 2009.
29 H. R. Allcock, F. C. Bissell and E. T. Shawl, *J. Am. Chem. Soc.*, 1972, **94**, 8603.
30 W. Clegg, G. M. Sheldrick, C. D. Garner and I. B. Walton, *Acta Crystallogr., Sect. B*, 1982, **38**, 2906.
31 I. Lindqvist, *Ark. Kemi*, 1950, **2**, 325.
32 B. Krebs, S. Stiller, K. H. Tytko and J. Mehmke, *Eur. J. Solid State Inorg. Chem.*, 1991, **28**, 883.
33 J. Marrot and J.-M. Savariault, *Acta Crystallogr., Sect. C*, 1995, **51**, 2201.
34 B. M. Gatehouse and P. Leverett, *J. Chem. Soc. A*, 1971, 2107.
35 R. Colton and J. C. Traeger, *Inorg. Chim. Acta*, 1992, **201**, 153.
36 J. Le Quan Tuoi and E. Muller, *Rapid Commun. Mass Spectrom.*, 1994, **8**, 692.
37 T.-C. Lau, J. Wang, R. Guevremont and K. W. M. Siu, *J. Chem. Soc., Chem. Commun.*, 1995, 877.
38 M. J. Deery, O. W. Howarth and K. R. Jennings, *J. Chem. Soc., Dalton Trans.*, 1997, 4783.
39 S. J. Dunne, R. C. Burns and G. A. Lawrance, *Aust. J. Chem.*, 1992, **45**, 1943.
40 S. J. Dunne, J. A. Irwin, R. C. Burns, G. A. Lawrance and D. C. Craig, *J. Chem. Soc., Dalton Trans.*, 1993, 2717.
41 A. L. Nolan, R. C. Burns, G. A. Lawrance and D. C. Craig, *J. Chem. Soc., Dalton Trans.*, 1996, 2629.
42 O. W. Howarth, P. Kelly and L. Pettersson, *J. Chem. Soc., Dalton Trans.*, 1990, 81.
43 M. J. Deery, T. Fernandez, O. W. Howarth and K. R. Jennings, *J. Chem. Soc., Dalton Trans.*, 1998, 2177.
44 G. A. Tsigdinos and C. J. Hallada, *Isopoly Compounds of Molybdenum, Tungsten and Vanadium*, Bulletin Cdb-14, Climax Molybdenum Company, New York, 1969.
45 D. L. Kepert, *Prog. Inorg. Chem.*, 1962, **4**, 199.